https://doi.org/10.5194/egusphere-2026-3860
Preprint. Discussion started: 17 July 2026
© Author(s) 2026. CC BY 4.0 License.

Observing Phase Transitions in Extreme Rainfall Events: Insights from Sub-Minute Observations and Universal Multifractal Analysis

Ching-Chun Chou[1,3], Auguste Gires[2], Ioulia Tchiguirinskaia[2], Daniel Schertzer[2,3], and Li-Pen Wang[1,3]

[1]Department of Civil Engineering, National Taiwan University, Taipei 10617, Taiwan
[2]HM&Co, École nationale des ponts et chaussées, Institut Polytechnique de Paris, Champs-sur-Marne, France
[3]Department of Civil and Environmental Engineering, Imperial College London, London SW7 2AZ, United Kingdom

Correspondence: Li-Pen Wang (lpwang@ntu.edu.tw)

Abstract. Complex systems across scientific disciplines often undergo abrupt, qualitative reorganizations –referred to as phase transitions– in which their fundamental properties change discontinuously. In geophysical contexts, such transitions can appear as sudden alternations in statistical behavior or scaling characteristics. In this study, phase transitions in extreme rainfall events are investigated through the Universal Multifractal (UM) framework, using ultra-high-resolution (10-second) disdrometer measurements collected during three typhoons in 2022: Hinnamnor, Nesat, and Nalgae. Two categories of multifractal phase transitions are examined: (i) transitions associated with sampling limitations and (ii) those related to moment divergence. While sampling limitations were observed during Typhoons Hinnamnor and Nesat, Typhoon Nalgae exhibited a clear case of moment divergence –a rare phenomenon indicative of extremely concentrated rainfall. These findings highlight the essential role of ultra-high-resolution time series in detecting and characterizing extreme hydrometeorological events. The study further demonstrates the capability of the UM framework to capture complex rainfall dynamics and offers insights that may contribute to improved hydrological modelling and flash-flood forecasting.

1 Introduction

Geophysical fields exhibit pronounced variability across a wide range of spatial and temporal scales. Understanding this variability and its associated extremes is fundamental for improving estimates of their impacts on human societies. The present study concentrates on extreme rainfall events induced by typhoons; however, the underlying methodology can be applied to other geophysical phenomena.

Extreme rainfall events –whose frequency and intensity are increasingly amplified by climate change– pose challenges worldwide owing to their abrupt onset, high magnitude, and spatially localized impacts, often triggering flash floods and landslides (Fowler et al., 2021). Accurately characterizing and predicting such events remains challenging due to their inherent complexity and multiscale variability. Furthermore, conventional observational systems tend to smooth sharp and intermittent features, leading to underestimation of rainfall extremes and distortion of their statistical structure. These deficiencies reduce the reliability of flood hazard assessments and limit the predictive capability of hydrological and water management models.

Accordingly, there is an increasing demand for high-resolution observational datasets and advanced analytical frameworks capable of resolving the fine-scale structure and dynamics of extreme rainfall. This study seeks to address this gap by employing

https://doi.org/10.5194/egusphere-2026-3860
Preprint. Discussion started: 17 July 2026
© Author(s) 2026. CC BY 4.0 License.

ultra-high-resolution rainfall measurements to examine the statistical characteristics of extreme events and to gain deeper insight into their complex behavior.

A promising approach to revealing such complexity lies in the study of phase transitions –abrupt and qualitative reorganizations in the dynamics of complex systems. Originally rooted in thermodynamics, the concept of phase transitions has been increasingly recognized in geophysical contexts, including atmospheric and hydrological systems (Bak, 1996). Within rainfall processes, these transitions may appear as sudden shifts in statistical properties or scaling behavior, potentially indicating the onset of extreme events or regime changes in rainfall dynamics. Investigating these transitions provides a deeper understanding of rainfall variability, complementing and extending conventional statistical descriptors.

The Universal Multifractal (UM) framework provides a theoretically robust means for analysing scale-invariant variability in geophysical processes such as rainfall (Schertzer and Lovejoy, 1987, 1997). Rooted in the physical concept of scale invariance –originating from the Navier-Stokes equations that describe atmospheric turbulence– the framework characterizes multiscale variability through three parameters. The *mean intermittency* (C_1) quantifies the average sparsity or intermittency of the field; the *multifractality index* (α) describes the degree of variability, distinguishing between 'mild' and 'wild' fluctuations; and the *non-conservative parameter* (H) measures the level of smoothness or departure from conservation within the field (Hubert, 2001; Veneziano et al., 2006; Lee et al., 2020). Altogether, these parameters describe how variability evolves with scale.

The UM framework is particularly well suited for analysing extreme rainfall, as it captures the heterogeneous distribution of rainfall intensity, including rare but high-magnitude events. It provides a mathematical formalism for describing scaling behavior and serves as a diagnostic tool for detecting phase transitions, such as the divergence of statistical moments or transitions constrained by data sampling (Mandelbrot, 1974; Chigirinskaya et al., 1994). In this study, the UM framework is applied to identify and characterize such transitions using ultra-high-resolution rainfall time series. The scaling moment function $K(q)$ and the two phase-transition criteria are defined formally in Sect. 2.2, with additional physical interpretation provided in Appendix A.

In summary, this study utilises ultra-high-resolution disdrometer observations from multiple typhoon events to explore the occurrence of phase transitions in extreme rainfall. The Universal Multifractal (UM) framework is employed to detect and quantify these transitions, with particular attention to moment divergence phenomena. Through this analysis, the study aims to advance understanding of rainfall variability across scales and to provide insights relevant for the prediction and management of extreme hydrometeorological events.

2 Data and method

2.1 Rain rate data

This study uses 10-second rainfall records collected by an OTT Parsivel^2 disdrometer installed at National Taiwan University –one of the highest temporal resolutions currently available (Park et al., 2017). This fine granularity captures short-lived and intermittent extremes that are often missed by coarser instruments. The quality of these records was verified against a collocated OTT Pluvio^2 weighing rain gauge, as detailed at the end of this section.

https://doi.org/10.5194/egusphere-2026-3860
Preprint. Discussion started: 17 July 2026
© Author(s) 2026. CC BY 4.0 License.

Table 1. Summary statistics of the trimmed rainfall time series for typhoons Hinnamnor, Nesat, and Nalgae in 2022. Timestamps are in UTC+0 time zone.

Event	Duration (hr)	Total (mm)	Max. Int. ($\mathrm{mm\,hr^{-1}}$)	Start – End
Hinnamnor	91.02	122.14	89.15	31-Aug 12:17 – 04-Sep 07:18
Nesat	45.51	191.57	103.52	14-Oct 22:50 – 16-Oct 20:20
Nalgae	91.02	70.14	30.92	28-Oct 22:54 – 01-Nov 17:55

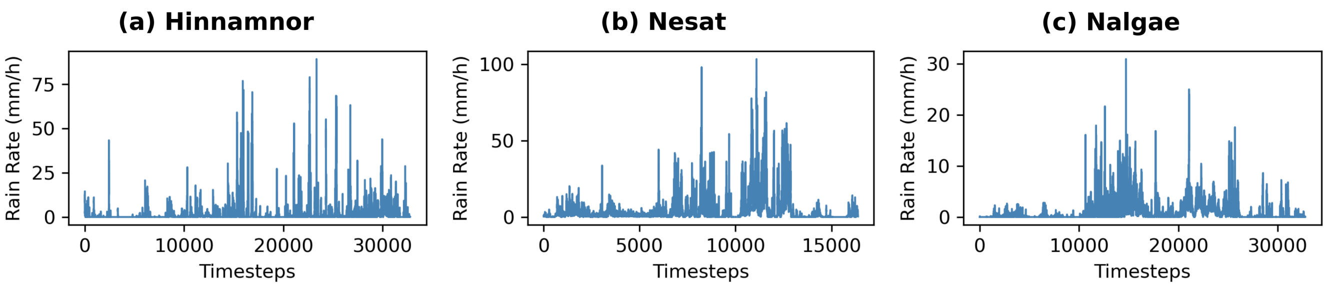

Figure 1. Typhoon rain rates recorded at 10-second intervals for the trimmed analysis periods of three typhoon events: (a) Hinnamnor, (b) Nesat, and (c) Nalgae. The corresponding start and end times are provided in Table 1.

Three typhoons –Hinnamnor, Nesat, and Nalgae– occurring between August and November 2022 were selected (Chou, 2025) for their substantial rainfall totals and the continuity of their high-resolution observations. To facilitate multifractal analysis, data were trimmed such that the number of data points corresponded to powers of two. A moving-window approach was applied to identify the segment with the highest cumulative rainfall for each event. The resulting trimmed segments, consisting of 32,768, 16,384, and 32,768 data points for Hinnamnor, Nesat, and Nalgae respectively, were used for analysis. This preprocessing ensured the creation of high-quality datasets suitable for accurate identification of phase transitions. A summary of these selected data segments is provided in Table 1, and the full time series are shown in Fig. 1.

The quality of the 10-second records was verified against the collocated OTT Pluvio^2 weighing gauge over the same trimmed segments. Because the gauge's real-time intensity channel cannot register rates below 6 $\mathrm{mm\,hr^{-1}}$, its threshold-free accumulation channel (Accu NRT, reported as depth per minute) was adopted as the reference; the comparison is accumulation-based, with the disdrometer intensities integrated to depth and the Accu NRT signal corrected for its fixed 7-minute processing delay (identified by cross-correlation). As the weighing gauge is itself a 1-minute, temporally smoothed measurement, 1 minute is the finest physically meaningful comparison scale. At this scale the disdrometer tracks the gauge closely (pooled Pearson $r = 0.94$, $R^2 = 0.88$), with agreement increasing monotonically to $r = 0.97$ ($R^2 = 0.94$) at 60-minute aggregation (Fig. 2); each event individually tracks the reference with $r = 0.96$–0.99 at 10-minute aggregation. The double-mass relationship is linear in every event, confirming that the disdrometer faithfully reproduces the temporal structure and relative distribution of rainfall intensity.

https://doi.org/10.5194/egusphere-2026-3860
Preprint. Discussion started: 17 July 2026
© Author(s) 2026. CC BY 4.0 License.

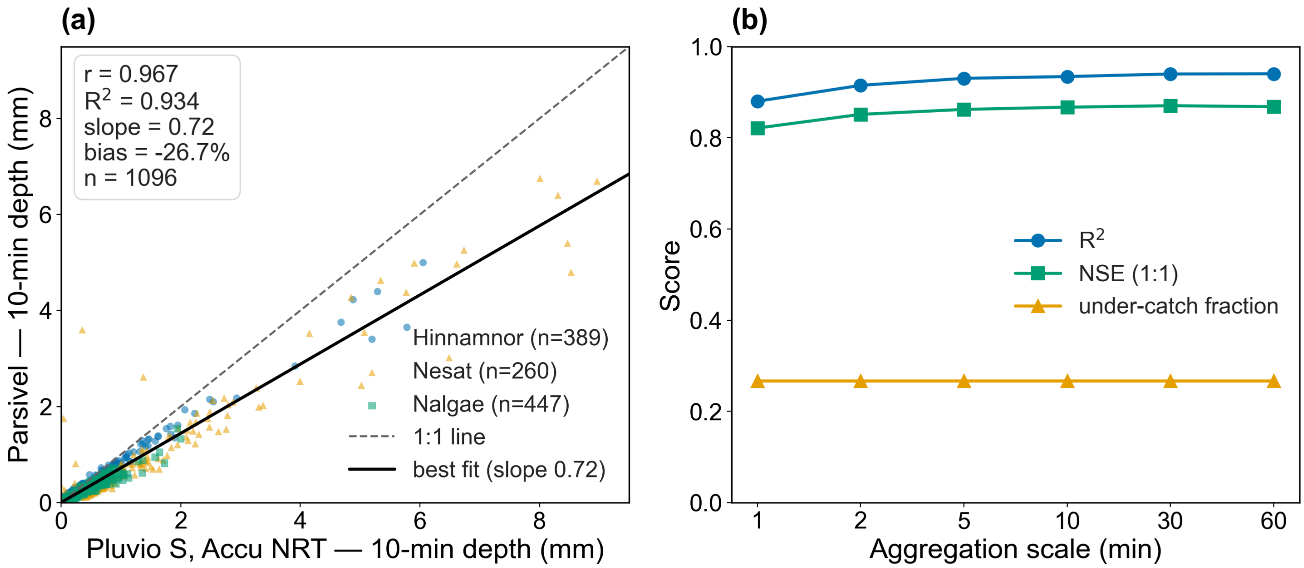

Figure 2. Validation of the 10-second disdrometer against the collocated Pluvio weighing gauge (Accu NRT channel), lag-corrected, over the analysed segments. (a) Pooled 10-minute rainfall depths for the three typhoons against the reference; the dashed line is 1:1 and the solid line the best fit through the origin. (b) Agreement metrics as a function of aggregation scale: the correlation (R^2) and Nash–Sutcliffe efficiency (NSE) increase with scale while the relative under-catch remains constant at $\approx 27\%$, confirming a multiplicative, scale-invariant bias.

The disdrometer underestimates the absolute rain amount, but the deficit behaves as a single multiplicative factor: the pooled relative bias is $\approx -27\%$ at every aggregation scale from 1 to 60 minutes (Fig. 2b) and is essentially uniform across intensity classes within each event. Such underestimation is well documented for laser disdrometers and does not affect the present analysis, because the UM parameters are derived from the normalized flux $\epsilon_\lambda = R_\lambda/\langle R_\lambda\rangle$ (Eqs. 5 and 10), which is invariant under multiplication of the field by a constant. Consequently α, C_1, and H – and the spectral exponent β, which depends on the slope rather than the amplitude of the power spectrum – are unchanged by the calibration offset; moreover, because the bias is intensity-independent it cannot preferentially distort the high-order moments and thus cannot generate the moment-divergence signature identified for Typhoon Nalgae. The raw 10-second series are therefore used throughout without bias correction.

2.2 Universal Multifractal framework

The Universal Multifractal (UM) analysis begins with a spectral analysis of the trimmed rainfall time series to evaluate the scaling behavior and to estimate the degree of non-conservation. When the power spectral density follows a power law with exponent $-\beta$,

$$E(k) \propto k^{-\beta}, \tag{1}$$

https://doi.org/10.5194/egusphere-2026-3860
Preprint. Discussion started: 17 July 2026
© Author(s) 2026. CC BY 4.0 License.

where $E(k)$ is the spectral energy and k the wavenumber, the field is scale-invariant. The spectral exponent β is related to the non-conservation parameter H through

$$\beta = 1 + 2H - K(2), \tag{2}$$

where $K(2)$ is the second-moment scaling exponent of the conservative component (Tessier et al., 1993). When non-conservative behavior is confirmed, the observed field ϕ_λ can be decomposed as

$$\phi_\lambda \approx \epsilon_\lambda \lambda^{-H}, \tag{3}$$

where ϵ_λ is a conservative field and λ the scale ratio. Fractional differentiation is applied to recover ϵ_λ from the original record (Tessier et al., 1993; Nykanen, 2008), thereby improving the consistency of the scaling regime across all subsequent analyses.

For a conservative field ϵ_λ observed at resolution $\lambda = L/l$ (outer scale L, observation scale l), the UM framework describes scale-dependent variability through two equivalent representations. The probability of exceeding a scale-dependent threshold λ^γ is governed by the co-dimension function $c(\gamma)$:

$$Pr(\epsilon_\lambda \geq \lambda^\gamma) \approx \lambda^{-c(\gamma)}, \tag{4}$$

where γ is the singularity order. The equivalent moment-scaling relation is

$$\langle \epsilon_\lambda^q \rangle \approx \lambda^{K(q)}, \tag{5}$$

where $K(q)$ is the scaling moment function, related to $c(\gamma)$ through a Legendre transform. Under the UM model, $K(q)$ takes the specific parametric form

$$K(q) = C_1 \frac{q^\alpha - q}{\alpha - 1}, \tag{6}$$

where C_1 is the mean intermittency and $\alpha \in (0,2]$ is the multifractality index. This two-parameter family captures the full range of multifractal behavior, from nearly monofractal fields ($\alpha \to 0$) to the most heterogeneous distributions ($\alpha = 2$). The theoretical form of $K(q)$ in Eq. (6) serves as the reference curve against which empirical departures – indicative of phase transitions – are identified.

Two types of phase transition are examined in this study, each manifesting as a characteristic departure of the empirical $K(q)$ from Eq. (6). The first arises from sampling limitations. Any finite dataset can only resolve singularities up to a maximum observable order γ_s, beyond which $K(q)$ becomes linear in q. The finite sampling dimension D_s is defined through $N_s = \lambda^{D_s}$,

https://doi.org/10.5194/egusphere-2026-3860
Preprint. Discussion started: 17 July 2026
© Author(s) 2026. CC BY 4.0 License.

where N_s is the number of independent samples, and γ_s is obtained from $c(\gamma_s) = D + D_s$, where D is the physical dimension of the system. The corresponding critical moment order q_s at which this linearisation occurs is

$$q_s = \left(\frac{D + D_s}{C_1}\right)^{1/\alpha}. \tag{7}$$

The second type of transition – moment divergence – reflects an intrinsic property of the field rather than a data limitation. When the underlying probability distribution decays as a power law,

$$Pr(\epsilon > x) \approx x^{-q_D}, \quad x \gg 1, \tag{8}$$

statistical moments of order $q \geq q_D$ are formally unbounded. In this regime, the empirical $K(q)$ exceeds the theoretical expression of Eq. (6), and the co-dimension function $c(\gamma)$ becomes linear for $\gamma > \gamma_D$. Such divergence, if detected, constitutes evidence that the rainfall field contains genuine extreme singularities rather than merely large but finite fluctuations.

The UM parameters α and C_1 are estimated using the Trace Moment (TM) and Double Trace Moment (DTM) techniques (Lavallée et al., 1993). The TM method evaluates the scaling of statistical moments with resolution by examining the log–log relationship

$$\log\langle\epsilon_\lambda^q\rangle \approx K(q)\log\lambda + \text{constant}, \tag{9}$$

where each moment order q yields a straight line with slope $K(q)$. The coefficient of determination r^2 at $q = 1.5$ is adopted as a representative indicator of scaling quality. The DTM method provides a more robust direct estimation of α and C_1 by raising the conservative field ϵ_λ at the highest available resolution Λ to the power η, forming a normalized transformed field $\epsilon_\lambda^{(\eta)} = [\epsilon_\Lambda(\mathbf{x})]^\eta / \langle[\epsilon_\Lambda(\mathbf{x})]^\eta\rangle$. Applying the TM method to $\epsilon_\lambda^{(\eta)}$ yields the scaling exponent function $K(q,\eta)$ for each η:

$$\langle\epsilon_\lambda^{(\eta)q}\rangle \approx \lambda^{K(q,\eta)} = \lambda^{K(q\eta) - \eta K(q)}. \tag{10}$$

Combining Eqs. (6) and (10) gives the theoretical relationship

$$K(q,\eta) = \eta^\alpha K(q), \tag{11}$$

so that for a fixed q, the slope of $\log K(q,\eta)$ versus $\log\eta$ directly yields α, and the intercept provides C_1. Further discussion of the physical interpretation of the UM framework is provided in Appendix A.

3 Results

Spectral analysis confirmed that the typhoon rainfall fields were initially non-conservative (see Fig. 3, top row), a behavior transformed after fractional differentiation was applied (see Fig. 3, bottom row). The estimated UM parameters are summarized

https://doi.org/10.5194/egusphere-2026-3860
Preprint. Discussion started: 17 July 2026
© Author(s) 2026. CC BY 4.0 License.

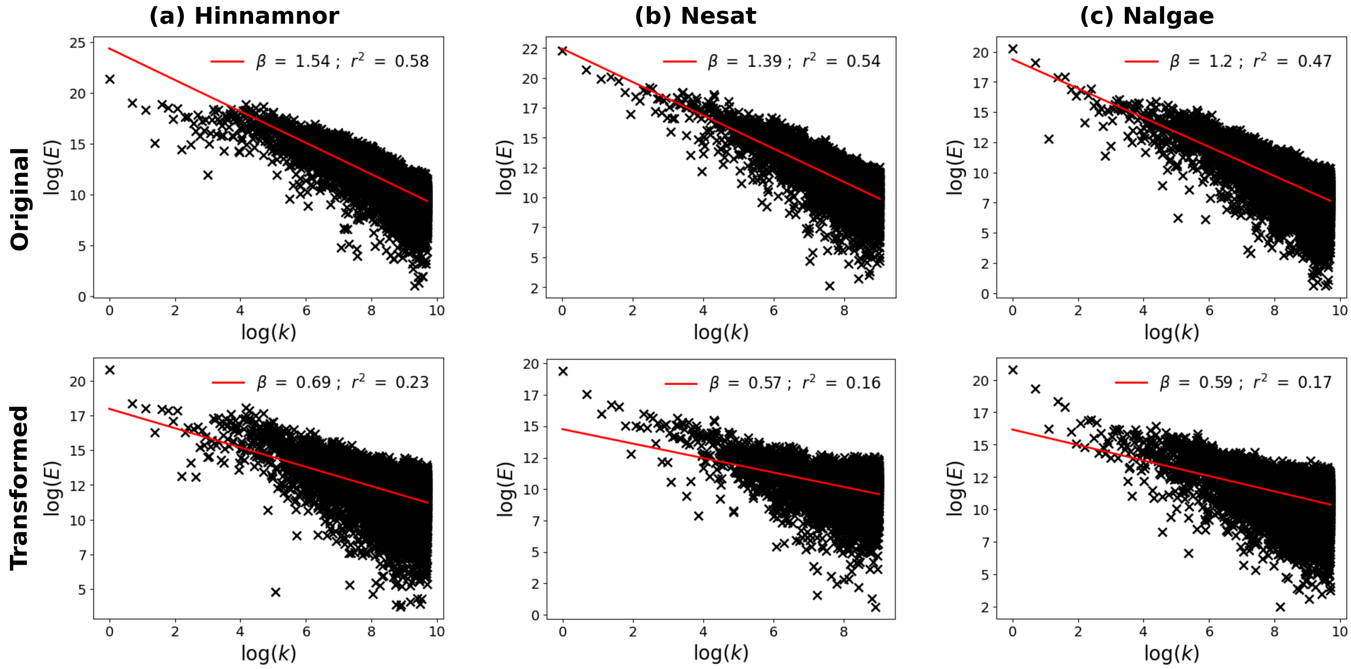

Figure 3. Spectral analysis of trimmed rainfall time series for (a) Hinnamnor, (b) Nesat, and (c) Nalgae. Top row shows the spectral analysis of the original fields, indicating their non-conservative nature. Bottom row shows the spectral analysis after applying fractional differentiation, which approximates the absolute value of the field's fluctuations. Each plot includes the spectral exponent β and the coefficient of determination r^2, highlighting the scaling behavior and the quality of fit for each typhoon event.

in Table 2 and the full scaling analysis is illustrated in Fig. 4. TM analysis (Fig. 4, top row) exhibited excellent scaling ($r^2 > 0.98$ for $q = 1.5$) across temporal scales from 10 seconds to 4 days, confirming that the power-law form of $\langle \epsilon_\lambda^q \rangle$ holds consistently and that the UM parameter estimates are reliable.

The $K(q)$ analysis (Fig. 4, bottom row) revealed two distinct types of multifractal phase transition, identifiable through characteristic departures of the empirical $K(q)$ from the theoretical form given by Eq. (6).

Typhoon Hinnamnor showed a linear departure of $K(q)$ at $q = 5.4$, characteristic of sampling limitations. The empirical transition order ($q_s^{\text{Emp}} = 5.4$) closely matched the theoretical value ($q_s^{\text{Theo}} = 5.0$) computed from Eq. (7) using the estimated UM parameters (see Table 2), indicating that finite-sample effects constrained robust estimation of higher-order statistical moments. The close agreement between q_s^{Emp} and q_s^{Theo} provides strong evidence that the observed departure is a sampling artefact rather than a genuine physical feature of the rainfall field. This has practical implications for rainfall measurement accuracy, particularly in radar-based observations where effective sample sizes are typically smaller than those achievable with point disdrometer records. Typhoon Nesat also exhibited a linear $K(q)$ departure at $q = 3.7$, but its empirical and theoretical transition orders ($q_s^{\text{Emp}} = 3.7$ and $q_s^{\text{Theo}} = 5.8$) were markedly less consistent, suggesting the influence of additional factors beyond sampling limitations, possibly related to the internal rainfall structure during this event.

https://doi.org/10.5194/egusphere-2026-3860
Preprint. Discussion started: 17 July 2026
© Author(s) 2026. CC BY 4.0 License.

Table 2. UM parameters and estimates for the typhoon events Hinnamnor, Nesat, and Nalgae. The estimates include the theoretical maximum singularity moment order (q_s^{Theo}), the empirical maximum singularity moment order (q_s^{Emp}), the empirical critical moment order (q_D^{Emp}), and the decay slope ($-m$). *NA* indicates that the corresponding transition type was not detected or was not applicable for that event.

Event	α	C_1	q_s^{Theo}	q_s^{Emp}	q_D^{Emp}	$-m$
Hinnamnor	0.99	0.20	5.0	5.4	*NA*	1.87–5.53
Nesat	1.21	0.12	5.8	3.7	*NA*	4.29–4.56
Nalgae	1.18	0.12	6.0	*NA*	3.7	2.95–4.41

In contrast, Typhoon Nalgae exhibited empirical $K(q)$ values exceeding the theoretical expression at $q = 3.7$, a behaviour incompatible with sampling limitations alone and indicative of moment divergence. According to Eq. (8), this implies that the underlying probability distribution of ϵ decays as a power law with exponent $q_D \approx 3.7$, such that moments of order $q \geq q_D$ are formally unbounded. This critical phase transition signifies the emergence of extreme singularities and a fundamental shift in the statistical character of the rainfall field, distinguishing Nalgae from the other two events. Such behaviour reflects exceptionally concentrated precipitation – a physical realization of the divergent-moment regime rather than a finite-sample limitation.

Power-law decay analysis of the empirical probability distributions further confirmed Nalgae's moment divergence (Fig. 5). Two dominant slopes were identified in each log-log plot. For Hinnamnor and Nesat, low R^2 coefficients across candidate slopes were consistent with the absence of a well-defined q_D, corroborating the interpretation that their $K(q)$ transitions were primarily driven by sampling limitations. In contrast, Nalgae exhibited markedly higher R^2 values for the steeper slope, consistent with the $K(q)$ analysis and indicating a stable power-law tail with $q_D \approx 3.7$. The strong mutual consistency between the $K(q)$ departure and the power-law decay analysis constitutes convincing evidence for true moment divergence during Typhoon Nalgae.

4 Conclusions

This study provides empirical evidence that multifractal phase transitions can occur in ultra-high-resolution rainfall records. Among the analysed typhoons, Nalgae exhibited moment divergence, indicating an abrupt shift in cascade dynamics and exceptionally concentrated rainfall. Hinnamnor and Nesat, by contrast, showed no divergence, illustrating how finite sampling can mask extreme singularities and that their absence in short records does not imply physical nonexistence.

The divergence observed in Nalgae reflects a genuine physical realization of unbounded rainfall intensity rather than a mathematical artifact. Such phase-like transitions reveal changes in rainfall organization beyond traditional statistical measures and offer a diagnostic marker for truly extreme events.

https://doi.org/10.5194/egusphere-2026-3860
Preprint. Discussion started: 17 July 2026
© Author(s) 2026. CC BY 4.0 License.

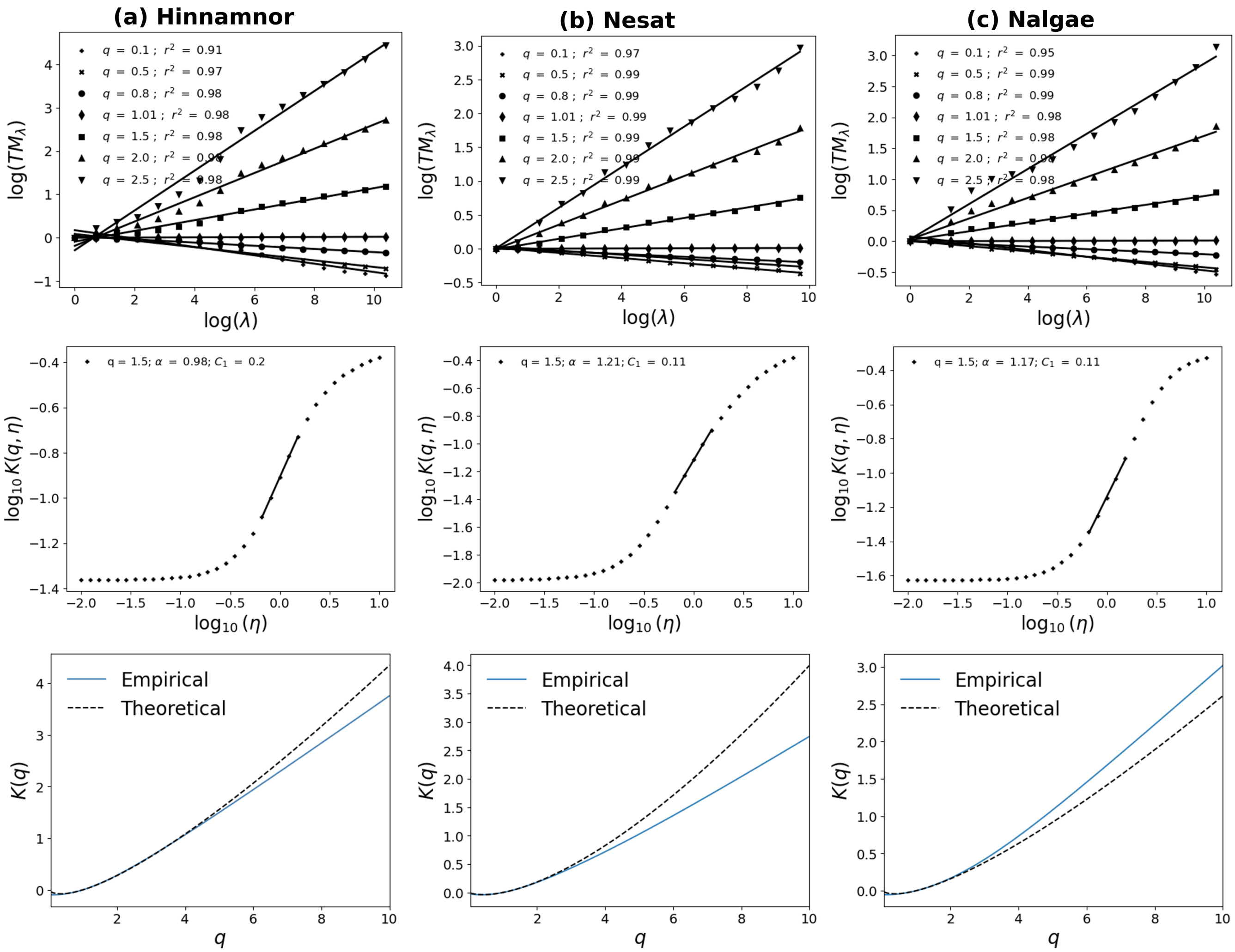

Figure 4. Scaling analysis and UM parameter estimation for (a) Hinnamnor, (b) Nesat, and (c) Nalgae. Top row: log-log plots of TM analysis for ϵ_λ, showing good scaling behavior across q-values. Middle row: UM parameters estimated using log-log plots of the DTM analysis at $\log_{10}(\eta) = 0$. Bottom row: comparison of empirical and theoretical $K(q)$ values for different q-values using DTM UM parameter estimates. Hinnamnor and Nesat have maximum singularity moment order q_s around 5.4 and 3.7 respectively, while Nalgae has a critical moment q_D around 3.7.

High-frequency observations were essential for detecting these behaviors. The 10-second disdrometer data captured fluctuations that coarser instruments typically smooth out, with implications for rainfall-runoff modelling and flood forecasting. Without such fine-scale calibration, radar products and hydrological models may underestimate peak intensities and short-lived surges.

https://doi.org/10.5194/egusphere-2026-3860
Preprint. Discussion started: 17 July 2026
© Author(s) 2026. CC BY 4.0 License.

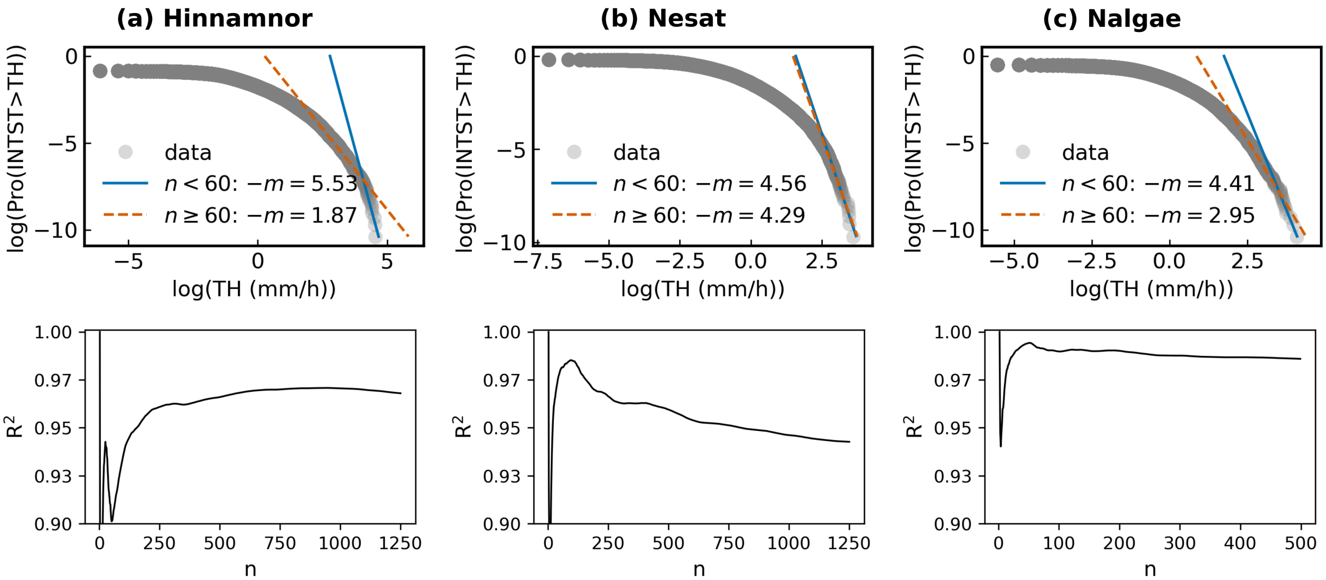

Figure 5. Top row: log-log plots of the empirical probabilities for rainfall time series (a) Hinnamnor, (b) Nesat, (c) Nalgae. The horizontal axis represents the normalized absolute value of fluctuations of the rainfall time series, and the vertical axis shows exceeding probabilities. Solid circles represent empirical values, the blue lines indicate best-fitting slopes for fewer than 60 data points, and red lines show optimal fits beyond this threshold. The coefficient of linear fitting (R^2) is plotted against the number of data points n for each typhoon, demonstrating fluctuations and identification of optimal slopes based on the R^2 criterion.

These findings demonstrate the value of applying the concept of phase transitions to rainfall and, more broadly, to other geophysical systems where abrupt scaling changes may expose underlying dynamics. Expanding analyses to longer and multi-site datasets will be crucial for assessing the prevalence of moment divergence under different climatic regimes and for refining theoretical models of multifractal variability.

Data availability. The disdrometer data used for Universal Multifractal analysis in this study are publicly available at Zenodo via https://doi.org/10.5281/zenodo.15378653 under an MIT License.

Appendix A: Universal Multifractal Framework: Physical Interpretation

The UM framework is rooted in the concept of multiplicative cascades, which model the redistribution of energy or flux across scales as a successive, scale-invariant multiplication process. Under common conditions, such cascades converge to the Universal Multifractal model, whose moment scaling function $K(q)$ takes the parametric form given by Eq. (6). The two parameters C_1 and α have distinct physical meanings. The mean intermittency C_1 controls the sparsity of the field: higher values imply

https://doi.org/10.5194/egusphere-2026-3860
Preprint. Discussion started: 17 July 2026
© Author(s) 2026. CC BY 4.0 License.

that the bulk of the measure is concentrated in an increasingly small fraction of the domain. The multifractality index α governs the rate at which extreme fluctuations amplify with increasing q: values near zero indicate a nearly uniform field (monofractal), while $\alpha = 2$ corresponds to log-normal cascades with the most heterogeneous singularity spectrum. Together, these parameters define the co-dimension function $c(\gamma)$ through the Legendre transform relating it to $K(q)$ (Eqs. (4)–(5)), which quantifies the fractal dimension of the set of singularities of order γ within the field.

The non-conservation parameter H in Eqs. (1)–(3) governs the smoothness of the field across scales. Physically, $H > 0$ corresponds to positively correlated increments (smoother fields with reduced small-scale variability), while $H < 0$ indicates anti-correlated increments and enhanced roughness. In the context of rainfall, positive H values are typical and reflect the physical persistence of precipitation intensity over short time intervals. Fractional differentiation, applied when H is significant, reverses this smoothing to yield a conservative field amenable to UM analysis.

A1 Phase transitions: physical interpretation

The two types of phase transition characterized in this study – sampling limitations and moment divergence – have distinct physical origins, both of which manifest as departures of the empirical $K(q)$ from the theoretical form of Eq. (6).

Sampling limitations (Eq. (7)) arise because any finite observational record constrains the range of detectable singularities. The maximum singularity γ_s observable within a dataset of N_s independent samples at resolution λ is determined by the sampling dimension D_s: larger datasets resolve higher singularities, and as the sample size decreases, the effective upper bound on γ contracts. Beyond γ_s, statistical estimates of $c(\gamma)$ and $K(q)$ become increasingly biased, and $K(q)$ linearises. This transition is a measurement artefact: it does not imply that the underlying field lacks extreme singularities, only that they are unresolvable with the available data. From a practical standpoint, this has direct implications for radar-based rainfall estimation, where effective sample sizes are generally far smaller than those achievable with high-frequency point measurements.

Moment divergence (Eq. (8)) is fundamentally different in character: it reflects a genuine property of the underlying multifractal measure. When the probability distribution of ϵ decays as a power law with exponent q_D, the statistical moments of order $q \geq q_D$ are formally infinite for the continuous cascade at infinite resolution. For any finite resolution λ, moments remain finite, but they grow without bound as $\lambda \to \infty$. This behaviour implies the existence of singularities of arbitrarily high order within the field – a physical realization of extreme concentration that cannot be dismissed as a finite-sample effect. In the scaling functions, this transition manifests as $K(q) \to \infty$ for $q > q_D$, and as a linear segment in $c(\gamma)$ for $\gamma > \gamma_D$. Empirically, moment divergence is identified through the combination of $K(q)$ values exceeding the theoretical expression and a well-defined power-law tail in the exceedance probability distribution with a stable decay slope and high R^2.

Author contributions. CC conceived the study, performed the analysis, and drafted the manuscript. AG and IT contributed to the theoretical framework and interpretation of results. DS provided expertise on multifractal theory and supervised the research. LW supervised the project, secured funding, and contributed to the manuscript revision. All authors read and approved the final manuscript.

https://doi.org/10.5194/egusphere-2026-3860
Preprint. Discussion started: 17 July 2026
© Author(s) 2026. CC BY 4.0 License.

Competing interests. Some authors are members of the editorial board of journal Nonlinear Processes in Geophysics.

220 *Acknowledgements.* This work was supported by the PRCI Ra2DW research project, jointly funded by the National Science and Technology Council (NSTC) under Grant No. 113-2923-M-002-001-MY4 and the Agence Nationale de la Recherche (ANR) under Grant No. ANR-23-CE01-0019-01. The authors acknowledge the financial support from the National Science and Technology Council (Taiwan) and the Agence Nationale de la Recherche (France).

https://doi.org/10.5194/egusphere-2026-3860
Preprint. Discussion started: 17 July 2026
© Author(s) 2026. CC BY 4.0 License.

References

Bak, P.: How Nature Works: The Science of Self-Organized Criticality, Springer New York, ISBN 978-1-4757-5426-1, 1996.

Chigirinskaya, Y., Schertzer, D., Lovejoy, S., Lazarev, A., and Ordanovich, A.: Unified multifractal atmospheric dynamics tested in the tropics: part I, horizontal scaling and self criticality, Nonlinear Processes in Geophysics, 1, 105–114, https://doi.org/10.5194/npg-1-105-1994, 1994.

Chou, C.-C.: Disdrometer Data used for UM analysis [dataset], https://doi.org/10.5281/zenodo.15378653, 2025.

Fowler, H. J., Lenderink, G., Prein, A. F., Westra, S., Allan, R. P., Ban, N., Barbero, R., Berg, P., Blenkinsop, S., Do, H. X., et al.: Anthropogenic intensification of short-duration rainfall extremes, Nature Reviews Earth & Environment, 2, 107–122, https://doi.org/10.1038/s43017-020-00128-6, 2021.

Hubert, P.: Multifractals as a tool to overcome scale problems in hydrology, Hydrological Sciences Journal, 46, 897–905, https://doi.org/10.1080/02626660109492884, 2001.

Lavallée, D., Lovejoy, S., Schertzer, D., and Ladoy, P.: Nonlinear Variability of Landscape Topography: Multifractal Analysis and Simulation, in: Fractals in Geography, Prentice Hall, https://www.physics.mcgill.ca/~gang/eprints/eprintLovejoy/neweprint/topoall.pdf, 1993.

Lee, J., Paz, I., Schertzer, D., Lee, D. I., and Tchiguirinskaia, I.: Multifractal Analysis of Rainfall-Rate Datasets Obtained by Radar and Numerical Model: The Case Study of Typhoon Bolaven (2012), Journal of Applied Meteorology and Climatology, https://doi.org/10.1175/JAMC-D-18-0209.1, 2020.

Mandelbrot, B. B.: Intermittent turbulence in self-similar cascades: divergence of high moments and dimension of the carrier, Journal of Fluid Mechanics, 62, 331–358, https://doi.org/10.1017/S0022112074000711, 1974.

Nykanen, D. K.: Linkages between Orographic Forcing and the Scaling Properties of Convective Rainfall in Mountainous Regions, Journal of Hydrometeorology, 9, 327–347, https://doi.org/10.1175/2007JHM839.1, 2008.

Park, S.-G., Kim, H.-L., Ham, Y.-W., and Jung, S.-H.: Comparative Evaluation of the OTT Parsivel^2 Using a Collocated Two-Dimensional Video Disdrometer, Journal of Atmospheric and Oceanic Technology, 34, 2059–2082, https://doi.org/10.1175/JTECH-D-16-0256.1, 2017.

Schertzer, D. and Lovejoy, S.: Physical modeling and analysis of rain and clouds by anisotropic scaling multiplicative processes, Journal of Geophysical Research: Atmospheres, 92, 9693–9714, https://doi.org/10.1029/JD092iD08p09693, 1987.

Schertzer, D. and Lovejoy, S.: Universal Multifractals Do Exist!: Comments on "A Statistical Analysis of Mesoscale Rainfall as a Random Cascade", Journal of Applied Meteorology and Climatology, p. 1296–1303, https://doi.org/10.1175/1520-0450(1997)036<1296:UMDECO>2.0.CO;2, 1997.

Tessier, Y., Lovejoy, S., and Schertzer, D.: Universal Multifractals: Theory and Observations for Rain and Clouds, Journal of Applied Meteorology and Climatology, 32, 223–250, https://doi.org/10.1175/1520-0450(1993)032<0223:UMTAOF>2.0.CO;2, 1993.

Veneziano, D., Langousis, A., and Furcolo, P.: Multifractality and rainfall extremes: A review, Water Resources Research, 42, https://doi.org/10.1029/2005WR004716, 2006.